J. Fluid Mech. (1992), *vol.* 234, *pp.* 121–146
Printed in Great Britain

A numerical simulation of the interaction of a compliant wall and inviscid flow

By ANTHONY D. LUCEY AND PETER W. CARPENTER
Department of Engineering, University of Warwick, Coventry, CV4 7AL, UK

(Received 15 June 1990 and in revised form 28 June 1991)

A method for numerically simulating the hydroelastic behaviour of a passive compliant wall of finite dimensions is presented. Using unsteady potential flow, the perturbation pressures which arise from wall disturbances of arbitrary form are calculated through a specially developed boundary-element method. These pressures may then be coupled to a suitable solution procedure for the wall mechanics to produce an interactive model for the wall/flow system. The method is used to study the two-dimensional disturbances which may occur on a Kramer-type compliant wall of finite length. Finite-difference methods are used to yield wall solutions driven by the fluid pressure after some perturbation from the equilibrium position. Thus, histories of surface deflection and wall energy are obtained. Such a modelling of the physics of the system requires no presupposition of disturbance form.

A thorough investigation of divergence instability is carried out. Most of the results presented in this paper concern the response of the compliant wall while (and after) a point pressure pulse, carried in the applied flow, travels over the compliant panel. Above a critical flow speed and once sufficient time has passed, the compliant wall is shown to adopt the particular profile of an unstable mode. After this divergence mode has been established, instability is realized as a slowly travelling downstream wave. These features are in agreement with the findings of experimental studies. The role of wall damping is clarified: damping serves only to reduce the growth rate of the instability, leaving its onset flow speed unchanged. The present predictions provide an improvement upon some of the unrealistic aspects of predictions yielded by travelling-wave and standing-wave treatments of divergence instability.

The response of a long compliant panel after a single-point pressure-pulse initiation, applied at its midpoint, is simulated. At flow speeds higher than a critical value, parts of the formerly (at subcritical flow speeds) upstream-travelling wave system change to travel downstream and show amplitude growth. The development of this 'upstream-incoming' wave illustrates how divergence instability can occur at locations upstream of the point of initial excitation. Faster flexural waves transmit energy upstream, thereafter these disturbances can evolve into slow downstream-travelling divergence waves. The spread of the instability to locations both downstream and upstream of the point of initial excitation indicates that divergence is an absolute instability. This behaviour and the effects of wall damping clarified by the present work strongly suggest that divergence is a Class C instability.

1. Introduction

There is now ample evidence, both experimental and theoretical, that significant postponement of laminar–turbulent transition can be achieved for boundary-layer

flow in water by using compliant walls. Much of this evidence is rather recent and is reviewed by Riley, Gad-el-Hak & Metcalfe (1988), Gad-el-Hak (1986*b*) and Carpenter (1990). In view of this evidence it is, perhaps, timely to progress from asking whether or not wall compliance can delay transition to seeking to maximize the delay. What, then, are the factors that limit the transition-delaying performance of compliant walls?

Hitherto there has been an understandable tendency to focus most of the attention on the effect of wall compliance on the Tollmien–Schlichting waves. However, the answer to the question posed above will not be found in this way. It is a fairly well-established fact, for example see figure 11 of Carpenter & Garrad (1985), that the Tollmien–Schlichting instability (TSI) could be completely stabilized if the wall were made sufficiently compliant. What prevents this stratagem from being successful in practice is the appearance of other types of instability – mainly hydroelastic (or wall-based) in nature. This point is very well illustrated by the empirical data obtained during the series of experimental tests carried out by Gaster (1987) and Daniel, Gaster & Willis (1987). The original experiments by Kramer (1960) on compliant coatings showed that substantial drag reductions, possibly attributable to transition delay, could be achieved. But the Gaster experiments firmly established for the first time that wall compliance could delay transition. Moreover, good agreement was found between the measured instability growth over the compliant walls and the theoretical predictions of Willis (1986). However, the transition process was quite different in the boundary layers over the compliant panels as compared to the rigid control. For instance, it appeared to be very much more sudden and violent. Precisely what happened in the transition process over the compliant walls remains unclear, but it is fairly certain that one of the other instability modes was involved. This point is discussed by Carpenter (1990) and Lucey, Carpenter & Dixon (1991).

Given that the interaction of two wave-bearing media, the fluid flow and the solid compliant wall, is involved, it is not surprising that many types of instability should be possible. This was well appreciated by Benjamin (1960, 1963) and Landahl (1962) who carried out the early theoretical studies on the stability of boundary layers over compliant walls. In order to make further progress towards the practical application of wall compliance for transition postponement, it is essential, as implied above, that these other types of instability be well understood. Two main types of hydroelastic, or flow-induced surface instability, have been observed for flows over compliant walls. These are *travelling-wave flutter* (TWF), which takes the form of a travelling wave with a phase speed close to the free-stream speed, and *divergence*, which either travels very slowly or is static. Travelling-wave flutter is amenable to the sort of theoretical treatment used for the TSI. In fact, a general asymptotic theory for this instability has recently been developed by Carpenter & Gajjar (1990). The present paper, on the other hand, is mainly devoted to a study of divergence, which requires a substantially different approach.

The mechanisms of destabilization for the TSI and TWF are rather subtle and both involve irreversible energy transfer which is made possible by phase shifts across the critical layer. In this respect divergence is much simpler. It occurs when a disturbance gives rise to hydrodynamic (pressure) forces which exceed the restorative forces in the compliant wall. This process primarily involves reversible energy transfer and, accordingly, one might expect any irreversible energy-transfer mechanisms, such as wall damping, to have a secondary effect. Despite this apparent simplicity, however, certain theoretical difficulties remain. The two main unresolved issues concern the role of wall damping – is it essential for the divergence instability?

– and the form taken by the instability – is it a travelling wave or a purely static instability? The conflicting evidence is briefly reviewed below.

The instability mechanism for divergence involves essentially conservative forces. Accordingly, to a reasonable approximation the wall may be regarded as being driven by hydrodynamic forces generated by an unsteady, purely potential, flow. Thus, a pessimistic, but probably fairly accurate, estimate of the onset speed for divergence may be found by using potential-flow theory to calculate the driving force and then solving the equation of motion for the wall. For an infinitely long surface a travelling-wave form may be assumed for the wall displacement, thereby reducing the problem to a dispersion equation for the complex phase speed. Such solutions, see for example Landahl (1962), Dugundji, Dowell & Perkin (1963), Duncan, Waxman & Tulin (1985) and Carpenter & Garrad (1986), predict that divergence appears in the form of a slow downstream-travelling wave, but only when wall damping is present. At higher flow speeds, divergence gives way to a more violent modal-coalescence flutter. In the absence of wall damping only the latter instability occurs. The fact that damping appears to be required for divergence has led many authors to suggest that, following the Landahl (1962)–Benjamin (1963) classification scheme, it is a Class A† instability like the TSI. However, Carpenter & Garrad (1986) have shown that the divergence instability has zero group velocity. This implies that it is an *absolute* instability, rather than a *convective* instability like TWF and the TSI. Accordingly, one would expect divergence to be Class C, implying that damping would have little influence on its onset.

The theoretical work based on potential flow has been briefly reviewed above. Some authors, however, have been able to incorporate viscous boundary-layer effects into their theoretical modelling of the divergence instability. Duncan *et al.* (1985), for example, introduced a semi-empirical correction to the wall pressure, p_{pot}, corresponding to potential flow, to approximate the actual wall pressure as

$$K_p \, \mathrm{e}^{\mathrm{i}\theta_p} p_{\text{pot}}.$$

For modelling divergence with a laminar boundary layer they obtained values of $K_p \approx 0.07$ and a phase shift of $\theta_p \approx -30°$ from the numerical simulations of Balasubramanian & Orszag (1983) for a boundary layer over a fixed wavy wall. The negative phase shift suggests that viscous effects exert a strong stabilizing effect. This is broadly in agreement with the more recent work of Evrensel & Kalnins (1988) who have been able to incorporate the viscous effects of the boundary layer in their numerical study. For compliant walls comprising a single homogeneous layer they found that the divergence mode is always stable for elastic or slightly viscoelastic walls, whereas for higher viscoelastic damping divergence was found in the form of growing waves travelling slowly downstream. The most complete investigation was carried out by Sen & Arora (1988). Their 'inverse' approach has the advantage of including all the possible modes of response. Divergence could be identified with their Kelvin–Helmholtz mode. For spring-backed tensioned-membrane walls they found that, except for very long waves at very low Reynolds number (based on boundary-layer thickness), the divergence instability only occurred for high wall damping.

Let us now consider the experimental studies of divergence. Of all the instabilities that might occur in the wall/flow system, divergence is the one that has been most consistently observed in experiments. Puryear (1962), Dugundji *et al.* (1963),

† *Class A(B)* waves are destabilized (stabilized) by wall damping and other similar irreversible energy-transfer processes. *Class C* waves are largely unaffected by irreversible energy exchange.

McMichael, Klebanoff & Mease (1979), Hansen & Hunsten (1974, 1983) and Gad-el-Hak, Blackwelder & Riley (1984) have all recorded divergence as an essentially two-dimensional instability. The measurement of drag in the rotating-disc experiments of Hansen & Hunsten (1974) emphasized the importance of 'designing-out' divergence, there being a marked increase in drag due to the roughness-like effect of the instability's spanwise ridges. The most comprehensive measurements of divergence have been made by Gad-el-Hak *et al.* for a turbulent boundary-layer flow over a homogeneous viscoelastic wall. At a clearly defined flow speed, divergence waves appear, travelling with phase speeds of approximately 5% of the surface shear-wave speed. Essentially two-dimensional in character, they come to occupy all streamwise locations of the surface, suggesting an absolute instability. A similar experiment was performed by Gad-el-Hak (1986*a*) but using an almost elastic wall; in this case divergence does not occur. Instead, the surface is destabilized by faster moving (50% of shear-wave speed) waves which may be identified with Class B TWF. The differences between the modes of destabilization of the two types of wall led Gad-el-Hak to surmise that surface-energy dissipation is a prerequisite for the occurrence of divergence.

A common pattern seems to emerge from the theoretical studies reviewed above. It would appear that substantial wall damping is required in order for the divergence instability to exist. This view is also in complete accordance with the experimental studies of Gad-el-Hak *et al.* However, this view has been questioned by Carpenter & Garrad (1986) who pointed out that, for the type of wall in question, which comprises a single viscoelastic layer, in the absence of damping the onset flow speed for TWF is lower than that for divergence. The onset speed for TWF rises quite markedly as the wall damping is increased. Accordingly, they argued that, since divergence appears to be an absolute instability, wall damping could not play an essential role in the destabilization process but, rather, removed the possibility of the TWF so that the experimenter only saw divergence.

However plausible this alternative explanation of the experimental observations might be in isolation, it still remains to explain why numerical studies, such as those by Evrensel & Kalnins (1988) and Sen & Arora (1988), which incorporate the full viscous boundary-layer effects, also indicate that substantial wall damping is required for divergence to appear. The explanation may be found in their assumption of an infinitely long surface. This is a perfectly good assumption for convective instabilities which are destabilized by irreversible energy transfer. But for an absolute instability, like divergence, involving essentially conservative forces the leading and trailing edges of the compliant panel may play a subtle but vital role in the destabilization process. This point certainly emerges from the work presented below, but it is studied analytically in more detail in Lucey (1989). The essential point can be understood by making reference to potential flow over an infinite compliant wall (for example, see Carpenter & Garrad 1986). In this case in the absence of damping a state of neutral stability exists for a range of flow speeds above the divergence-onset speed. The fact that the wave travels slowly downstream keeps the destabilizing hydrodynamic forces in equilibrium with the restorative forces in the wall. The inclusion of wall damping, however light, breaks this equilibrium and allows the divergence wave to grow. For a wall of finite length the effect of the leading and trailing edges, however distant, also breaks this equilibrium thereby allowing divergence to grow even in the absence of damping. For this reason any theoretical or numerical model of divergence, which is based on the assumption of an infinitely long surface, omits a vital ingredient in the destabilization process and is

liable to lead to misleading conclusions, particularly with regard to the effects of wall damping.

There are a number of studies of hydroelastic instability for potential flow over finite panels. For example, see Weaver & Unny (1971), Ellen (1973) and Garrad & Carpenter (1982). In all these studies divergence occurs in the absence of damping. In fact, Garrad & Carpenter were able to predict both the onset speed and critical wavelength for divergence on walls of the type used by Kramer (1960). Moreover, their predictions were in good agreement with the experimental observations of Puryear (1962). However, all the studies referred to above are based on the arbitrary assumption that the instability takes the form of standing waves. Attempts have been made to reconcile the differences between the travelling-wave (infinite surface) and the standing-wave (finite surface) approaches. For example, Carpenter & Garrad (1986) have conducted an asymptotic investigation of a finite surface in the limit of infinite wavenumber. They demonstrated that both methods give the same onset speed. Nevertheless, the differences between the two approaches with regard to damping and the predicted forms of the instability remain unresolved. What is required is a method of modelling divergence on a compliant wall of finite length which makes no assumption about the initial or subsequent forms of the disturbance.

The method used in the present paper meets the above requirement. It uses a novel treatment of the hydrodynamics based on a boundary-integral formulation.† This allows numerical simulations of a wide variety of initial-value problems to be undertaken. In this respect our work is more like an experimental investigation than a theoretical study. At present the hydrodynamics is restricted to potential flow, although the method of Duncan *et al.* (1985), referred to above, may be used to take the boundary-layer effects into account in an approximate fashion. Plainly, it would be highly desirable to incorporate the full viscous effects. This would, however, be an extremely challenging computational problem. Domaradzki & Metcalfe (1987) and Metcalfe *et al.* (1991) have carried out direct numerical simulations of the linear and nonlinear development of disturbances in boundary layers over compliant walls. The viscous effects are fully incorporated but these are temporal calculations for an infinite surface based on the assumption of periodic inflow and outflow. Thus, a truly spatial calculation for a *finite* compliant surface may well be beyond the state of the art. Our method may, however, be readily extended to three-dimensional finite panels.

2. Computational model

The mechanics of the disturbed wall/flow system may be represented by an equation of motion written in the form

$$\mathrm{L}w = -\delta p(\ddot{w}, \dot{w}, w) \tag{2.1}$$

subject to initial values and surface-edge conditions. L is a differential operator on the vertical surface displacement, w, and δp is the pressure perturbation due to the disturbances to the free-stream flow, U_∞. Coordinate axes are as shown in figure 1. For Kramer-type walls, a fluid substrate may be present; this feature is not included in the present work. It is known, see Garrad & Carpenter (1982), that an inviscid substrate contributes an additional inertial term to the system, whilst Carpenter & Garrad (1985) have shown that a viscous substrate generates a term which operates

† A somewhat similar method has been independently developed by D'Sa & Dalton (1990).

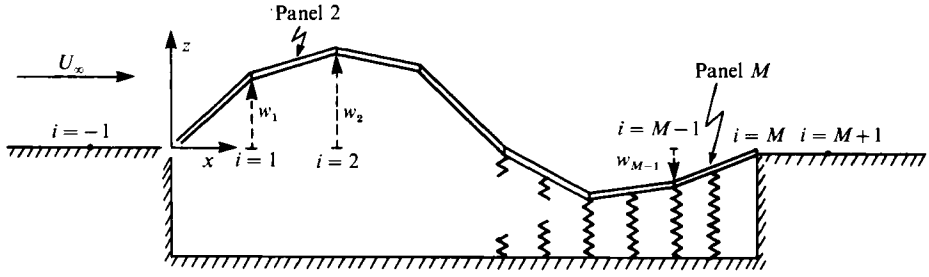

FIGURE 1. A schematic illustration of the compliant wall showing the discretization of the surface into boundary elements.

in a similar fashion to structural damping. For the anticipated low phase speeds associated with divergence waves, the magnitude of this added inertia allows it to be neglected in the interests of simplicity.

2.1. *Wall mechanics*

In the case of the plate–spring representation of a Kramer-type surface, then

$$\mathrm{L}w \equiv \rho_{\mathrm{m}} h \frac{\partial^2 w}{\partial t^2} + d\frac{\partial w}{\partial t} + \left(B\frac{\partial^4}{\partial x^4} + K_{\mathrm{E}}\right) w, \tag{2.2}$$

where ρ_{m}, h and B are respectively the density, thickness and flexural rigidity of the plate. K_{E} is the equivalent spring stiffness, consisting of the spring stiffness and the body-force coefficients, whilst d is the coefficient of structural damping of the wall. The flexural rigidity is related to the elastic modulus, E, and the Poisson ratio, ν, as follows:

$$B = \frac{Eh^3}{12(1-\nu^2)}.$$

The flexible surface is discretized into a set of boundary elements or panels, $m = 1, 2, \ldots, M$. Interior mass points, $i = 1, 2, \ldots, (M-1)$, at which the mechanical properties of the wall will be assumed centred, are defined by the panel end-points. The discretized form of (2.1), having used (2.2), at time level t is

$$\rho_m h \ddot{w}_i^t + d\dot{w}_i^t - [B\,\partial^4/\partial x^4 + K_{\mathrm{E}}]\, w_i^t = -\delta p_i^t, \tag{2.3}$$

where

$$\left[B\frac{\partial^4}{\partial x^4} + K_{\mathrm{E}}\right] w_i^t = \left(\frac{6B}{(\delta x)^4} + K_{\mathrm{E}}\right)(w_i^t) - \frac{4B}{(\delta x)^4}(w_{i+1}^t + w_{i-1}^t) + \frac{B}{(\delta x)^4}(w_{i+2}^t + w_{i-2}^t). \tag{2.4}$$

Throughout this work hinged-edge conditions will be used. Thus, zero deflection and zero turning moment at the leading and trailing edges are imposed; when using centred differences, the following constraints apply:

$$w_{-1} = -w_1 \quad \text{and} \quad w_{\mathrm{M+1}} = -w_{\mathrm{M-1}}.$$

However, it would be simple to apply other conditions, such as 'built-in' edges which specify zero surface slope at the leading and trailing edges. It is noted that both the finite-difference form of the flexural stiffness and the edge boundary conditions require that 'dummy' mass points, additional to the interior mass points, are required. Thus we have that $i = -1, 0, 1, 2, \ldots, (M+1)$, although the solution procedure will only need to consider the interior points.

2.2. *Fluid mechanics*

In order to compute the unsteady hydrodynamic pressures due to arbitrary surface disturbances, a boundary-integral method of flow solution is employed. This method is well-known in the aerospace industry and is documented in the seminal article of Hess & Smith (1966). Its mathematical formalism is recorded in Hunt (1978). Nevertheless, some details of how this method was adapted for the current problem are noted below.

Disturbances to the free-stream flow are characterized by the velocity-perturbation potential, $\Phi(x, z, t)$; this function can be found by spreading a singularity distribution over the wall/flow boundary and then applying the condition of zero flux across the (moving) wall/flow interface. Thus:

$$\nabla\Phi \cdot \boldsymbol{n} + \boldsymbol{U}_\infty \cdot \boldsymbol{n} = u_S, \tag{2.5}$$

where $\boldsymbol{n}$ is an outward-pointing normal vector and u_S is the speed of the moving surface in the normal direction. In this work, the singularities chosen as solutions to Laplace's equation are source(−sink) lines. The perturbation potential is therefore

$$\Phi(\boldsymbol{r}) = \frac{1}{2\pi}\int_l \sigma(\boldsymbol{r}_S)\ln|\boldsymbol{r}-\boldsymbol{r}_S|\,\mathrm{d}s, \tag{2.6}$$

where $\boldsymbol{r}$ is the location of any point in the semi-infinite space above the wall and $\boldsymbol{r}_S$ is the locus vector of the wall which maps out the wall/fluid interface, l. The source-strength function is denoted $\sigma(\boldsymbol{r}_S)$. Substitution of (2.6) into the boundary condition, (2.5), leads to the following equation which defines the source strength distribution:

$$\tfrac{1}{2}\sigma(\boldsymbol{r}) + \frac{1}{2\pi}\frac{\partial}{\partial n}\left\{\int_{\substack{l \\ \boldsymbol{r}_S \neq \boldsymbol{r}}} \sigma(\boldsymbol{r}_S)\ln|\boldsymbol{r}-\boldsymbol{r}_S|\,\mathrm{d}s\right\} + \boldsymbol{U}_\infty \cdot \boldsymbol{n} = u_S, \tag{2.7}$$

where the singularity at $\boldsymbol{r} = \boldsymbol{r}_S$, seen in (2.6), has been properly treated. The surface is now modelled as a collection of panels (i.e. line segments) as shown in figure 1; if the source strength, σ, is assumed constant over each panel, then (2.7) becomes

$$\tfrac{1}{2}\sigma_i + \sum_{\substack{m=1 \\ m\neq i}}^{M} \sigma_m\left\{\frac{1}{2\pi}\int_{\text{panel } m} \frac{\partial}{\partial n_i}(\ln|\boldsymbol{r}_i-\boldsymbol{r}_m|)\,\mathrm{d}s\right\} + \boldsymbol{U}_\infty \cdot \boldsymbol{n}_i = u_{S_i} \tag{2.8}$$

for $i = 1, 2, \ldots, M$. It is now noted that this form represents a set of M linear equations for the unknowns, σ_i. The system may be solved and the appropriately discretized form of (2.6) used to determine the perturbation potential on the surface. Subsequently, through the use of the unsteady Bernoulli equation, the pressure on the surface may be found.

The terms in braces in (2.8) are recognized as being influence coefficients and are seen to be dependent solely upon the interface geometry. In the unsteady problem this geometry evidently changes; thus, at every time step of the evolving disturbance the influence coefficients would have to be recalculated and a possibly large matrix would have to be inverted in the solution of the linear system, (2.8). Both of these requirements would be computationally expensive. This, together with the fact that the representation of surface mechanics is confined to the linear regime, suggests that a more economical variant of the boundary-element technique be used. A linear version has been developed. This requires that: (i) the sources/sinks for each panel will be presumed to lie in the plane $z = 0$ and not on the displaced surface, (ii) the

source strength of a particular panel will be determined solely by that panel's streamwise orientation and its normal velocity; and (iii) second-order terms in angles, displacements and flow-speed perturbations will be neglected.

The consequences of these assumptions are that the geometry-dependent influence coefficients remain unchanged throughout the motion, needing only to be calculated once, and the system of equations which determine the panel source/sink strengths decouple, thereby reducing to the set of equalities:

$$\sigma_i = 2(U_\infty \alpha_i + U_{s_i}), \tag{2.9}$$

where α_i is the panel's angle to the horizontal and U_{s_i} is its vertical speed.

In order to assess the limitations of the linear method, both the nonlinear and linear boundary-integral methods have been coded and tested against each other. A fundamental sinusoidal deflection is imposed upon the surface, the ratio of amplitude to half-wavelength (equivalent to a thickness ratio) of which can be varied. When this ratio is 0.1 then the hydrodynamic-stiffness distribution calculated by each of the two methods is almost identical; for a ratio of 0.25, the linear method overestimates the hydrodynamic stiffness by approximately 10%. Thus, for the small deflections associated with the linear regime of divergence instability, and consistent with the linear model adopted for the wall mechanics, the use of the linear method is regarded as acceptable.

For (idealized) modal deflections, semi-analytical methods (e.g. Ellen 1973; Garrad & Carpenter 1982) are available for the calculation of the generalized hydrodynamic stiffnesses that result from the Galerkin approach (see Dowell 1975) to the hydroelastic analysis of finite surfaces. Equivalent generalized forces may be calculated using the present flow solution by carrying out a numerical integration over the number of panels present in the discretization. These may be compared with the equivalent semi-analytical results to determine the resolution (of the surface into a collection of panels) required to meet an acceptable level of accuracy. Testing of the numerical model for the compliant panel *in vacuo*, using sinusoidal disturbances has shown that a resolution of six panels per half-wavelength yields standing waves with a frequency of oscillation accurate to 2%. In contrast, the linear boundary-element method requires in excess of twenty panels to reproduce such accuracy in the square root of hydrodynamic stiffness. Thus, a first-order boundary-element method, using linearly varying source strengths over each panel, has been developed to enhance the flow solution. This is a standard technique, see Hess (1973), and, in the present context, for a discretization of six panels per half-wavelength, gives the square root of the hydrodynamic stiffness within 3% of that found using semi-analytical methods. This order of accuracy is now commensurate with that given by the finite-difference scheme for the wall mechanics and thus further improvements to the flow solution have not been sought.

A suitable form of the unsteady hydrodynamics is now developed. The discretized form of the linearized unsteady Bernoulli equation is

$$\delta p_i = -\rho U_\infty u_i - \rho \frac{\partial \Phi_i}{\partial t}. \tag{2.10}$$

Velocity perturbations and perturbation potentials on the surface are given by

$$u_i = \sum_{m=1}^{M} (\sigma_m I_{im}^S + \lambda_m I_{im}^H), \quad \Phi_i = \sum_{m=1}^{M} \sigma_m I_{im}^\Phi, \tag{2.11 a, b}$$

where I^S_{im}, I^H_{im} and I^Φ_{im} are sets of time-independent influence coefficients and σ_m is the source strength at the panel centre (control point) with λ_m being the coefficient of the linear variation over the panel m. Panel angles and normal velocities are given by

$$\alpha_i = \frac{w_i - w_{i-1}}{\delta x_i}, \quad U_{s_i} = \frac{\dot{w} + \dot{w}_{i-1}}{2}. \tag{2.12a, b}$$

Using the source strength definitions given by (2.9), then (2.10), (2.11) and (2.12) may be combined to give that

$$\delta p_i(w, \dot{w}, \ddot{w}) = \delta p_i^{S1}(w) + \delta p_i^{S2}(\dot{w}) + \delta p_i^{U1}(\dot{w}) + \delta p_i^{U2}(\ddot{w}), \tag{2.13}$$

where

$$\delta p_i^{S1}(w) = 2\rho U_\infty^2 \sum_{m=1}^{M} \left\{ \left(\frac{w_m - w_{m-1}}{\delta x} \right) I^S_{im} + \lambda_m I^H_{im} \right\}, \tag{2.14a}$$

$$\delta p_i^{S2}(\dot{w}) = 2\rho U_\infty \sum_{m=1}^{M} \left\{ \left(\frac{\dot{w}_m + \dot{w}_{m-1}}{2} \right) I^S_{im} \right\}, \tag{2.14b}$$

$$\delta p_i^{U1}(\dot{w}) = 2\rho U_\infty \sum_{m=1}^{M} \left\{ \left(\frac{\dot{w}_m - \dot{w}_{m-1}}{\delta x} \right) I^\Phi_{im} \right\}, \tag{2.14c}$$

$$\delta p_i^{U2}(\ddot{w}) = 2\rho \sum_{m=1}^{M} \left\{ \left(\frac{\ddot{w}_m + \ddot{w}_{m-1}}{2} \right) I^\Phi_{im} \right\}. \tag{2.14d}$$

The form of (2.13) clearly illustrates the physical significance of the decomposed unsteady pressure. The first term is the hydrodynamic stiffness which will determine the actual onset flow speed of divergence instability. The following two are normally termed the hydrodynamic damping, being conservative forces which modify the phase speed of surface waves. The fourth term is the hydrodynamic inertia which modifies the speed of the vertical oscillatory motion of the compliant wall.

The discretization implied in the above requires that all the surface panels are of identical length (hence δx has been written instead of δx_i). For most other applications, discretizations are chosen so that a finer resolution exists in regions of high curvature thus enabling accurate calculation of the hydrodynamic stiffness. In the present work such preconditioning is undesirable since wall deflections of arbitrary shape are to be accommodated. Accordingly, it is appropriate that a uniform grid be applied, although the resolution of arbitrary disturbances in the discretization scheme must be considered in estimating the accuracy of representation of such disturbances when they arise.

2.3. *Computational model for the interactive system*

The hydrodynamic pressures, given by (2.13), are evaluations at the control points of the surface panels. Simple averaging between adjacent panels is used to determine the value at the mass points utilized in the finite-difference scheme for the wall. The coupled wall/flow system is assembled by introducing these pressures into the right-hand side of the equation of motion for the wall, (2.3). Some manipulation of the defining equation is then required owing to dominance of the hydrodynamic inertia over the structural inertia. Thereafter, a semi-implicit method of solution, using Gauss–Seidel sweeps over the internal mass points, is used to yield converged values of acceleration, velocity and displacement for every mass point and at each time step in the evolution of the disturbed system. A detailed description and discussion of the numerical technique can be found in Lucey (1989).

3. Results and discussion

The computational model is now used to conduct a series of 'numerical experiments'. In order to investigate the behaviour the wall/flow system, some form of initial excitation is required. A wide variety of initial-value problems can be studied using the present model – see Lucey (1989). Here, we have chosen to concentrate upon the compliant-wall response to a point pressure pulse which may be travelling in the flow, §3.1, or take the form of an isolated 'hammer blow' at some point on the surface, §3.3. In §3.2 attention is given to the effects of damping on divergence instability. Perhaps the chief difficulty in using the present numerical simulation is identifying true hydroelastic instabilities as distinct from the flexural response of the wall to the above-mentioned forms of excitation. After the input of energy by the activating pressure pulse, visual evidence of disturbance growth at some location on the compliant wall may be deceptive since this could result from a localized concentration of the wall energy rather than arising from a transmission of fluid energy into the wall. We have therefore introduced a procedure which calculates the total wall strain energy, E_S kinetic energy, E_K and total energy, E_T ($= E_S + E_K$), as the wall response evolves. An additional useful quantity is the virtual work done by the hydrodynamic stiffness in the establishment of the disturbance at a particular time, W_V. These energies are evaluated using the following expressions:

$$E_S = \sum_{i=1}^{M-1} \left(\tfrac{1}{2} B w_i \frac{\partial^4 w_i}{\partial x^4} + \tfrac{1}{2} K_E w_i^2 \right) \delta x, \tag{3.1}$$

$$E_K = \sum_{i=1}^{M-1} \tfrac{1}{2} \rho_m h \dot{w}_i^2 \, \delta x, \tag{3.2}$$

$$W_V = \sum_{i=1}^{M-1} \tfrac{1}{2} w_i \left(\frac{\delta p_{i+1}^{S1} + \delta p_i^{S1}}{2} \right) \delta x. \tag{3.3}$$

Using these quantities, a true hydroelastic instability is identified by a sustained growth in the E_S and it first occurs when $W_V > E_S$. The second condition simply states that the (summed) destabilizing fluid forces must exceed the restorative structural forces within the wall for a hydroelastic instability to exist in the conservative system.

Throughout §§3.1 and 3.2, the material properties of the wall are those associated with the compliant coatings used in the experiments of Kramer (1960). These coatings have been the subject of discussion and analysis by Carpenter & Garrad (1985, 1986) and values of material properties extracted which are relevant to the plate–spring model. Thus, elastic modulus $E = 0.4 \times 10^6$ N/m^2 and equivalent spring stiffness $K_E = 230E$ N/m^3, the values for Kramer's softest coating, are chosen together with a plate thickness and density of 2 mm and 952 kg/m^3; the fluid density is taken to be 1000 kg/m^3. The methods of Garrad & Carpenter (1982) show that these will yield a critical (with regard to divergence) sinusoidal mode, $A_n \sin(n\pi x/a)$, with wavelength 0.0115 m. For computational convenience, a surface discretized into 60 panels is used in §§3.1 and 3.2. In order to give a resolution of six panels per half wavelength for the anticipated critical mode, a surface length, a, capable of accurately supporting five wavelengths ($n = 10$) of disturbance gives that $a \approx$ 0.06 m. This length may seem absurdly short by comparison with Kramer's original 0.94 m compliant surface. However, Garrad & Carpenter (1982) have also shown that for the higher-order modes with $n > 7$, the surface behaves very much like a surface

of infinite length in the generation of hydrodynamic forces. That is, the influence of leading and trailing edges is sufficiently reduced for it no longer to be regarded as the classic problem of panel instability. Of course, the present model could be used to give an exact simulation of Kramer's wall by using a discretization of approximately 1000 panels; however, little quantitative and qualitative gain would be conferred at the expense of a vastly increased computing time. When the surface motion is initiated by a deflection perturbation, then the initial (maximum) amplitude is chosen to be one hundredth of the half-wavelength of the anticipated most dangerous mode, with $n = 10$, so ensuring that the linear assumptions in both the fluid and structural mechanics are not violated.

3.1. *Travelling pressure-pulse initiation of wall motion*

A point pressure pulse is allowed to travel across the finite compliant wall in the (mean) free-stream flow. The pulse originates as a perturbation, ΔU, to the free-stream flow speed. This is incorporated by modifying the boundary-element method which is able to accommodate a spatially dependent onset flow speed. The undisturbed (by surface perturbations) flow field now becomes U', where

$$U'(x) = U_\infty - \delta(x - U_\infty t)\,\Delta U, \tag{3.4}$$

and δ is the Dirac delta function. A point pressure pulse is used rather than one with some built-in shape characteristic because any predisposition of the wall to a particular disturbance form is undesirable. It is hoped that the deflection profile will evolve solely from the physics of the system.

Figure 2(*a*) chronicles the wall response for the period during which the pulse is exciting the wall. The resulting deformations are seen to be flexural and the apparent periodicity is determined by the position of the pulse as it moves across the surface. Some time after the pulse has departed the trailing edge, the wall adopts the profiles seen in figure 2(*b*); disturbance growth is evident and the instability form is of a downstream-travelling wave which may be identified as divergence. Perhaps of greatest interest is that the system has 'found' a critical mode, this being the one for which $n = 10$ in a sinusoidal approximation of the wall deflection. The energy record for times covering those of figure 2(*a*) through to those of figure 2(*b*) is presented in figure 2(*c*). It is noted that the W_V exceeds the E_S in a sustained manner after 0.008 s have elapsed. Thus, divergence instability only occurs after a suitable surface deflection has been established. Further illustration of the instability form is given in figure 2(*d*) which was obtained at a flow speed of 20 m/s. These defections pertain to times after the pressure pulse has left the compliant wall. Away from the leading and trailing edges, the profile of the divergence mode is seen to be closely sinusoidal, the absence of flexural harmonics indicating the potency of the instability at this flow speed. The general form taken by divergence instability (seen in figures 2*a* and 2*d*), as a slowly travelling downstream wave, is in agreement with the experimental findings of Gad-el-Hak *et al.* (1984) who investigated the interaction between a finite compliant panel and an applied flow. The travelling-wave form of divergence is also demonstrated in the rotating-disc experiments of Hansen & Hunsten (1974, 1983). Gad-el-Hak *et al.* made careful measurements of the divergence wave, describing the wave profile as having sharp peaks with wide separating valleys and having an amplitude comparable to the thickness of the compliant coating. Such a profile is not obtained in the present work because we are using a different wall model – a spring-backed flexible plate rather than a viscoelastic slab – and our predictions are restricted to the linear regime of the development of divergence instability. The large

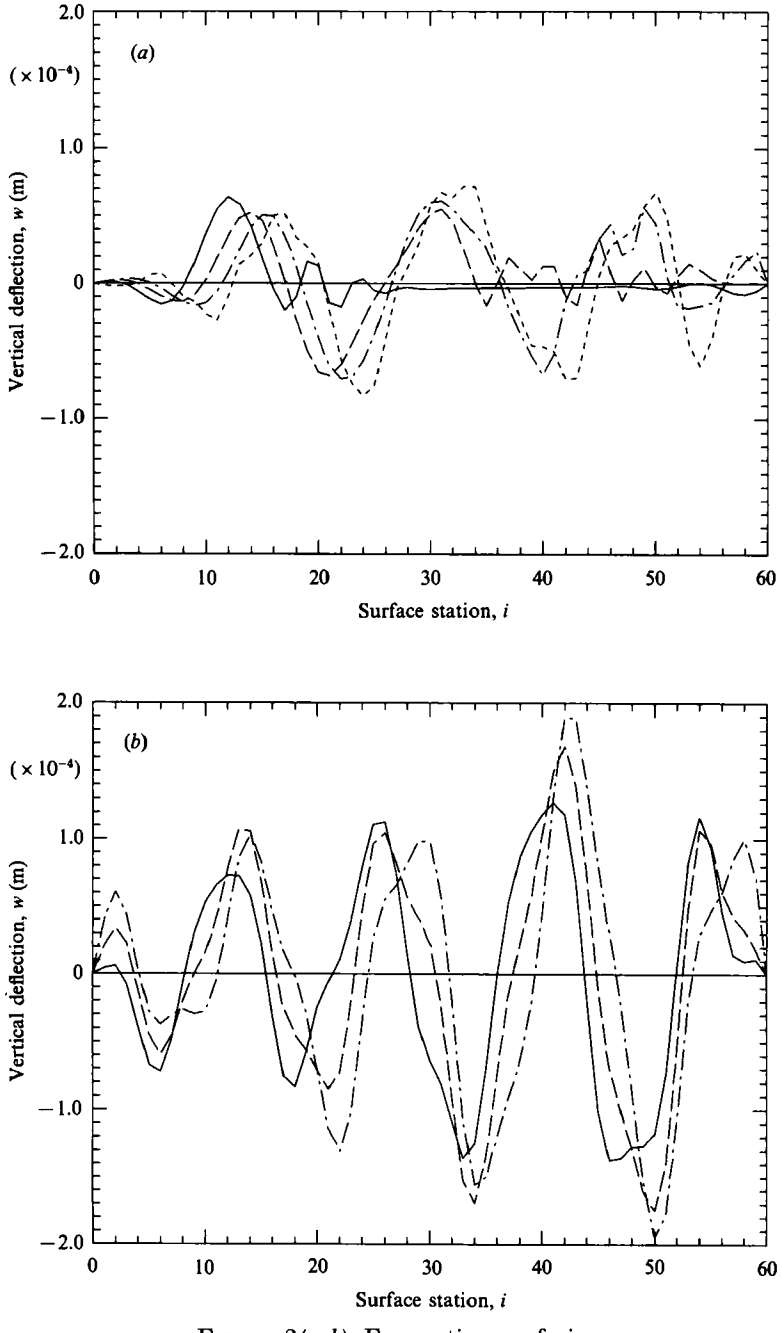

FIGURE 2(*a*, *b*). For caption see facing page.

amplitudes of the divergence wave, recorded in the experiments of Gad-el-Hak *et al.* strongly suggest that structural nonlinearities had come into play so halting further growth of the wave.

Three important points arise from the above results regarding divergence instability: (i) it is found in the absence of wall damping; (ii) it takes the form of a slow downstream-travelling wave; (iii) instability only occurs after the wall has

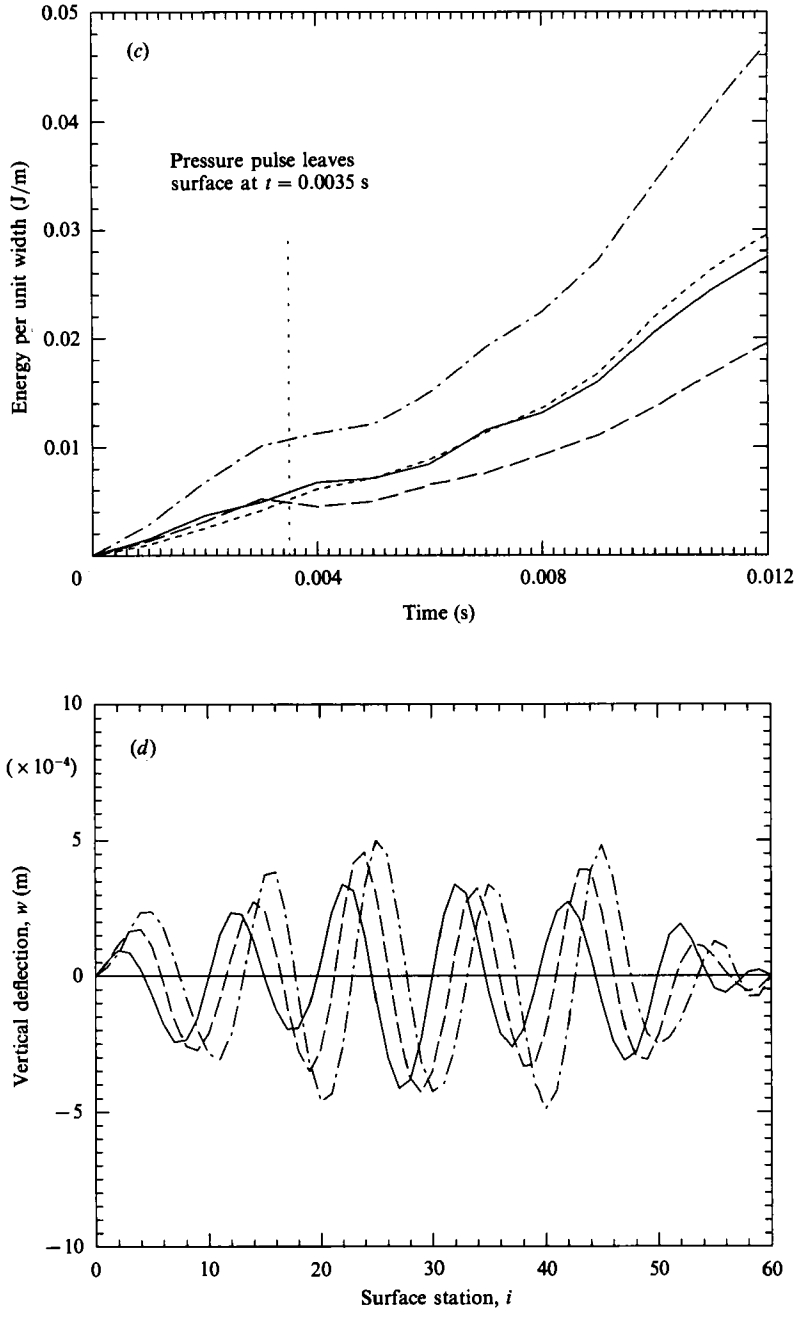

FIGURE 2. Wall response during and after a travelling pressure-pulse excitation. Wall data: $E = 0.4 \times 10^6$ N/m^2, $K_E = 230\,E$ N/m^3, $a = 0.06$ m, $h = 0.002$ m, $\rho_m = 952$ kg/m^3 and $d = 0$. The fluid density is 1000 kg/m^3. The variation of vertical wall deflection with wall-station number when $U_\infty = 17.5$ m/s: (*a*) at early times, surface position at: —, $t = 0.001$ s; ——, $t = 0.002$ s; –·–, $t = 0.003$ s; – – –, $t = 0.004$ s; (*b*) at later times (the pressure pulse left the compliant wall at $t = 0.0035$ s.), surface position at: —, $t = 0.010$ s; ——, $t = 0.011$ s; –·–, $t = 0.012$ s. (*c*) The variation of wall-energy with time: —, E_S; ——, E_K; –·–, E_T; – – –, W_V. (*d*) The variation of vertical wall deflection with wall-station number when $U_\infty = 20$ m/s, (the pressure pulse left the compliant wall at $t = 0.0030$ s.), surface position at: —, $t = 0.0050$ s; ——, $t = 0.0051$ s; –·–, $t = 0.0052$ s.

taken up the profile of a particular (or critical) mode. Regarding the onset flow speed of divergence, the present method shows good agreement with the analytical predictions of both standing-wave methods (e.g. Weaver & Unny 1971; Ellen 1973; Garrad & Carpenter 1982) and travelling-wave methods (see Landahl 1962; Dugundji *et al.* 1963; Carpenter & Garrad 1986) when the critical mode is used as the basis for the spatially dependent part of the wall deformation. However, important differences between the present predictions and those of each of the analytical methods exist.

Standing-wave methods predict a truly static instability even at flow speeds higher than that of onset. In the present work, divergence is only found to be a static phenomenon exactly at the onset flow speed. A detailed comparison of the two methods has been carried out by Lucey (1989). At sub-critical flow speeds, both methods predict that for a fully developed disturbance (i.e. one occupying all locations of the compliant panel) the wall response is dominated by upstream-travelling waves. In this regime it is found that $W_V < E_S$. These waves would therefore be quickly attenuated by wall damping and may be regarded as Class B flexural waves. Exactly at the critical flow speed, both methods find that $W_V = E_S$ at all times and thus static equilibrium exists. However, in the divergence regime of flow speeds the predictions are different. The standing-wave wave solution shows $W_V = E_S$ at $t = 0$, the two quantities then increasing as time passes, with W_V slightly in excess of E_S. Furthermore, the profile of the unstable mode is dependent upon the flow speed used. This suggests that the standing-wave method finds the particular *static* deflection with the highest E_S that may be destabilized at that flow speed. In fact, there may be could be numerous alternative deflection profiles with lower values of E_S that would also be unstable. In contrast, the present numerical method always shows energy records, within this same regime, with $W_V > E_S$ at $t = 0$. ($W_V = E_S$ only at the lowest flow speed for which divergence can occur.) The excess of hydrodynamic energy being transferred to the wall (over and above that which would cause the wall deflection to grow in a static configuration) forces the disturbance to travel downstream with a particular phase speed so that the energy-transfer excess is cut back to such a level that a sustained instability growth continues to occur. The present, more realistic, travelling-wave form, therefore, evinces lower growth rates than the equivalent static instability predicted by standing-wave methods.

In view of the above paragraph, it might seem that when making analytical predictions, the travelling-wave formulation is more appropriate. However, this approach can be misleading with regard to the effect of wall damping; this is discussed in the following subsection. Lastly, the surface behaviour at subcritical flow speeds should be mentioned although results are not presented here. These are dominated by seemingly random flexural effects after the pulse has left the surface. The complexity of the wall response is largely due to the repeated reflection of the flexural waves at the surface edges and the following wave interactions. It may be important to take such motions into account as it is these Class B flexural waves, when they travel downstream, which could support the existence of TWF. This may well be the critical instability when the effects of the boundary layer are taken into account.

3.2. *The effects of wall damping*

The effect of surface-energy dissipation has remained, perhaps, the most contentious aspect of divergence instability. In the analysis of a wall of finite length, it can be shown that when a single-mode (in retrospect, a reasonable simplification given the results presented above) solution is carried out, the only effect of wall damping is to reduce the growth rate of the instability leaving its onset flow speed unchanged. In

contrast, travelling-wave methods predict that divergence occurs once the flow speed for which the wave phase speed is identically zero has been exceeded, and only provided that there is damping present. Thus, proponents of the standing-wave approach would support the view that divergence is a Class C instability whilst those of travelling-wave methods are inclined to regard it as Class A.

To investigate the effects of wall damping in the present context, it is necessary to assign suitable values to the coefficient of damping, d, in (2.2). A damping factor, q, is introduced which is appropriate to standing-wave oscillations of the wall *in vacuo*. This is simply the ratio of the amplitudes at a single surface point separated in time by one period of oscillation. Thus, if the nth mode of a disturbance $A_n \sin(n\pi x/a) \exp(\mathrm{i}\omega t)$, where ω is the angular frequency of oscillation, is used in (2.1) with $\delta p = 0$, it is found that

$$d = -\frac{\ln q}{\pi}\left[B\left(\frac{n\pi}{a}\right)^4 + K_{\mathrm{E}}\right]^{\frac{1}{2}}(\rho_{\mathrm{m}} h)^{\frac{1}{2}}. \tag{3.5}$$

In using this formulation, the test values given to q are 0.75, 0.5 and 0.25 which represent a wide range of damping values.

Although the above-described formulation engenders a clear physical feeling for the amounts of damping to be introduced, it does represent a somewhat arbitrary approach as regards a true model of the effects of damping for Kramer's compliant coatings. It is therefore worthwhile relating the values inferred above to the data available for Kramer's natural-rubber walls. In fact, little definitive data is available for Kramer's original coatings; nevertheless, Carpenter & Garrad (1985) have collated and discussed such information that there is. The most important point to note is that the damping of Kramer's coatings was viscoelastic and so more properly modelled by a loss factor, η, which may be a complicated function of the wall motion's frequency. Complex elastic modulus and equivalent spring-foundation stiffness can be written

$$E^* = E_{\mathrm{r}}(1-\mathrm{i}\eta'), \quad K_{\mathrm{E}}^* = K_{\mathrm{E_r}}(1-\mathrm{i}\eta'') \tag{3.6a, b}$$

where the suffix r denotes the real part. If the loss factors for the above two components of the wall structure are taken as equal, then the out-of-phase term obtained from the use of (3.6a, b) in the equation of motion may be related to an equivalent coefficient of damping, expressed in (3.5), by

$$d \equiv \left[\frac{E_{\mathrm{r}} h^3}{12(1-\nu^2)}\left(\frac{n\pi}{a}\right)^4 + K_{\mathrm{E_r}}\right]\frac{\eta}{\omega}, \tag{3.7}$$

where it has been taken that $\eta = \eta' = \eta''$.

Using the present wall data and $n = 10$, *in vacuo* results for ω give that when $q =$ 0.75, 0.5 and 0.25, then $\eta = 0.092$, 0.221 and 0.441 respectively. If the angular frequency of vibration at zero flow speed is used then for $q = 0.75$, 0.5 and 0.25 the associated loss factors are $\eta = 0.065$, 0.157 and 0.313 respectively. It is appreciated that because of the absence of hydrodynamic stiffness at zero flow speed, these values represent the inferred top limits of η for a given q. Carpenter & Garrad deduce that the loss factors for the Kramer (1960) walls are less than or equal to 0.1. Thus, the proposed values of equivalent damping used here lie within an acceptable range.

To investigate the effect of damping on a compliant wall undergoing divergence instability, a set of runs at 17.5 m/s has been carried out for $q = 1.0$ (undamped), 0.75, 0.5 and 0.25. Since it has been shown (see figure 2b) that the critical mode for

this wall being used can be approximated by $A_n \sin(n\pi x/a)$ with $n = 10$, we have imposed this deflection on the compliant wall to serve as an initial perturbation. The wall is released at $t = 0$ and the disturbance evolution, for the undamped case ($q = 1.0$), is shown in figure 3(*a*). Deflection histories for the damped cases are not presented here because they are almost identical to figure 3(*a*) – only at the highest level of damping ($q = 0.25$) can a slight reduction in the growth rate of the instability be perceived. Instead, the energy records of all four cases are presented in figure 3(*b*). Only the values of E_S and W_V are plotted since $E_K \approx 0$ for this slowly travelling wave. In all cases, the growth of both E_S and W_V indicate that divergence instability is underway. The single effect of damping is to reduce the growth rate of the instability as compared with the result for the undamped wall. This is a clear indication of Class C behaviour. The primary mechanism for divergence instability is the reversible transfer of energy into the surface by conservative hydrodynamic forces. The removal of surface energy serves only to modify slightly the effect of the primary cause. Nor is the onset flow speed of divergence changed since precisely at the critical flow speed, the wall is in a state of static equilibrium.

This result runs counter to those of the travelling-wave methods for predicting divergence on an infinitely long wall which suggest that divergence cannot occur in the absence of wall damping. Landahl (1962) first described how damping precipitated divergence instability in the case of an infinitely long surface. The onset flow speed of divergence is determined by the value at which the originally upstream-travelling wave reverses to travel downstream. In an undamped system with no (surface) end constraints, neutral stability is maintained for flow speeds in excess of the critical flow speed because the so-called hydrodynamic damping (part of the potential-flow forcing given by (2.13)) is able to modulate the phase speed (and hence the relative flow speed) such that the hydrodynamic stiffness continues exactly to balance the restorative structural forces. This situation may be thought of as an unstable equilibrium which is broken by the introduction of damping. The phase speed of the wave is marginally reduced and the increase to the relative flow speed produces a hydrodynamic stiffness that is able to overcome the restorative forces and so instability ensues. The exact balance, which gives neutral stability, can only exist on an infinitely long surface where there is no structural impediment to wave travel. However, on any finite surface (in the absence of damping), it is the existence of leading and trailing edges which breaks the above balance. Previous authors (e.g. Landahl 1962, Dugundji *et al.* 1963; Duncan *et al.* 1985; Carpenter & Garrad 1986) have noted that any amount of damping, no matter how little, gives rise to instability of the slow downstream wave. So it is with leading- and trailing-edge effects; no matter how distant they may be from a centrally located disturbance, their marginal interference with totally free wave travel ensures that instability sets in immediately the originally upstream wave begins to travel downstream.

Attention has been given to the violent modal-coalescence flutter that both standing-wave and travelling-wave methods predict to replace divergence instability at higher flow speeds. From results not presented here, the current method shows that this evolves smoothly from divergence as the flow speed is increased. In agreement with the predictions of both standing-wave and travelling-wave theories, the growth rates of this severe instability are marginally reduced with damping. This is clearly Class C behaviour. In the absence of damping, this instability has been predicted by travelling-wave theories (e.g. Carpenter & Garrad 1986; Duncan *et al.* 1985) to be explosive in its onset, arising from the merging of two neutrally stable modes; only when damping was included did its evolution from divergence become

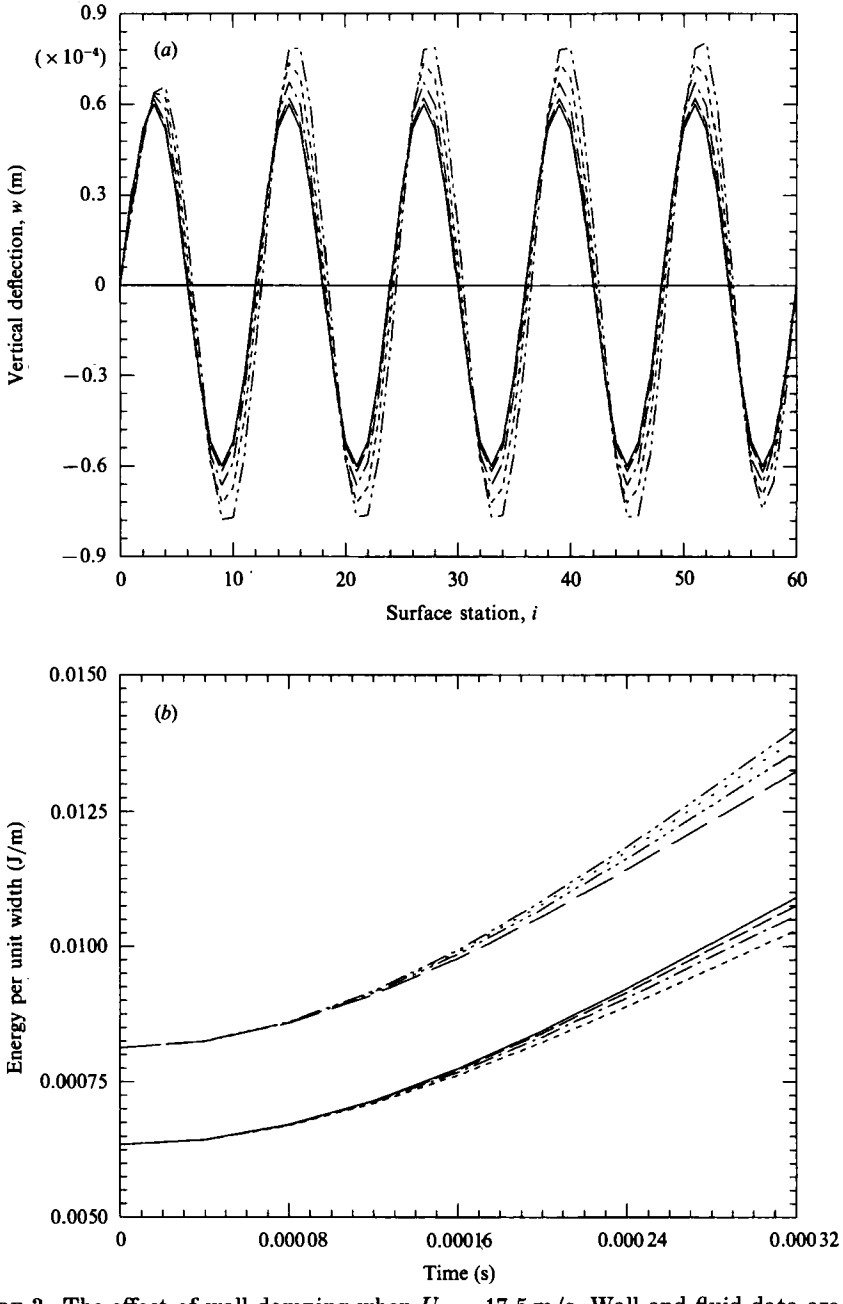

FIGURE 3. The effect of wall damping when $U_\infty = 17.5$ m/s. Wall and fluid data are as for figure 2. (*a*) The variation of vertical wall deflection with wall-station number for $q = 1.0$. Surface position at: —, $t = 0$ s; ——, $t = 0.00008$ s; –·–, $t = 0.00016$ s; – – –, $t = 0.00024$ s; –···–, $t = 0.00332$ s. (*b*) The variation of E_s and W_v with time for different values of the damping factor, q. E_s; —, $q = 1.0$ (undamped); ——, $q = 0.75$; – –, $q = 0.50$; – – – –, $q = 0.25$. W_v; –···–, $q = 1.0$ (undamped); ....., $q = 0.75$; –···–, $q = 0.5$; ——, $q = 0.25$.

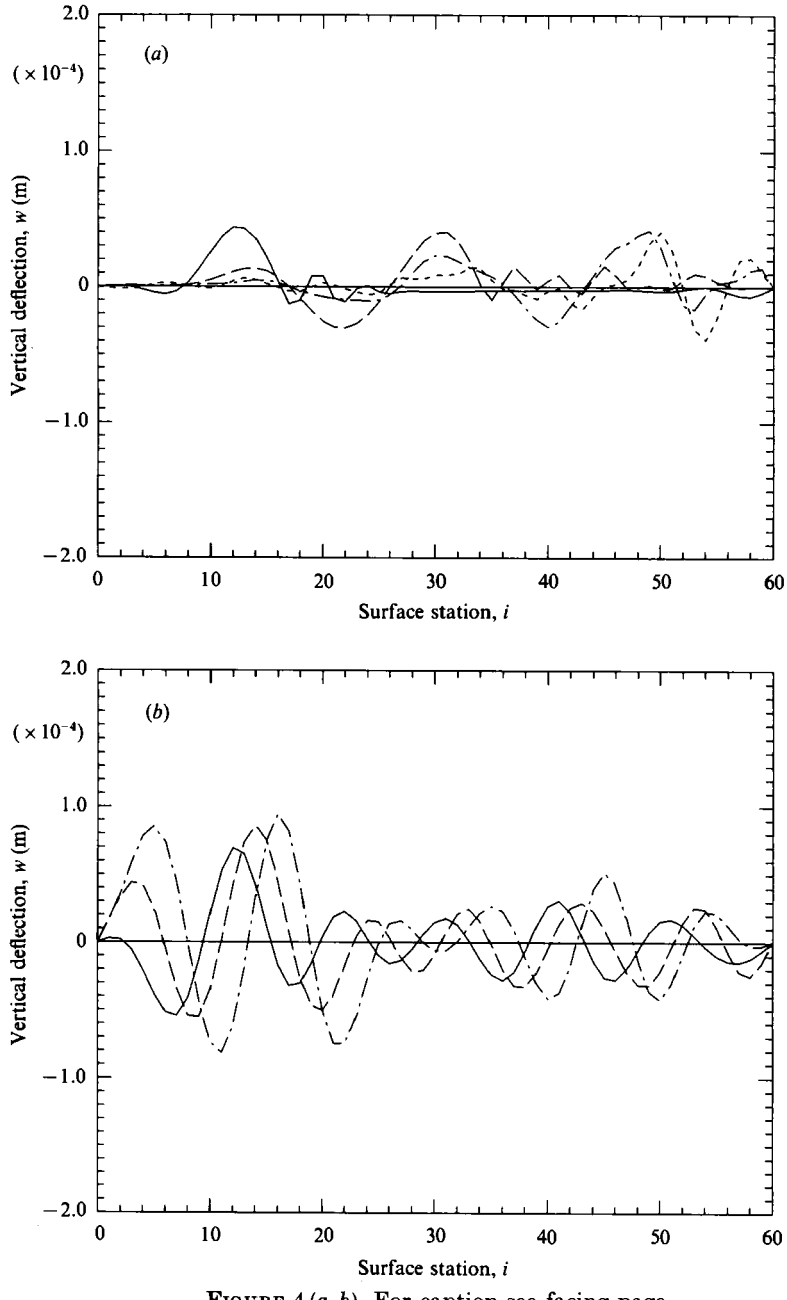

FIGURE 4(*a*, *b*). For caption see facing page.

smooth. In the present model its evolution from divergence instability is smooth even in the absence of damping. This suggests that the influence of edge effects on walls of finite length is somewhat similar to that of damping on infinitely long compliant walls.

Some results pertaining to the behaviour of a damped compliant wall over which a point pressure pulse passes are now presented. In the divergence range of flow speeds, figures 4(*a*) and 4(*b*) respectively chronicle the wall response whilst the pressure pulse is still on the surface and at later times when the divergence mode has

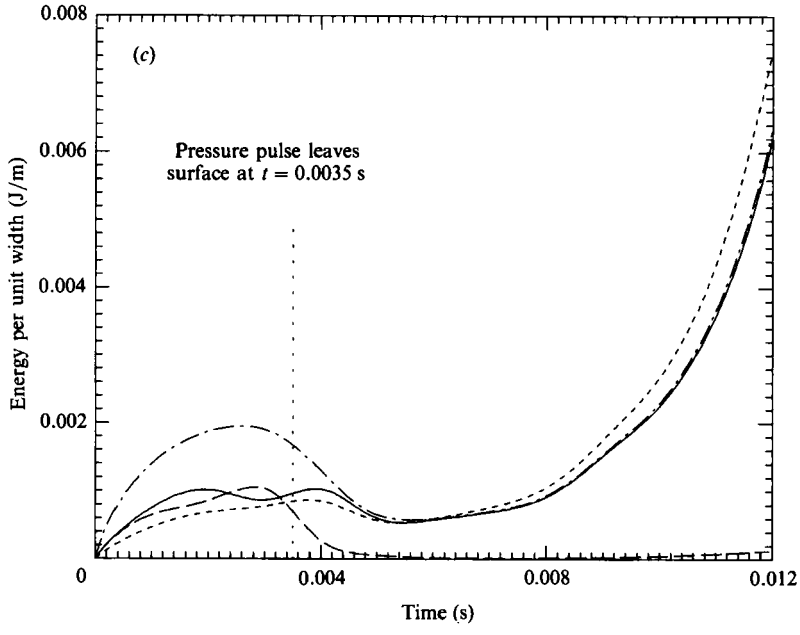

FIGURE 4. Damped-wall response during and after a travelling pressure-pulse excitation when $U_\infty = 17.5$ m/s. The damping factor, q, is 0.5 and the wall and fluid data are as for figure 2. (*a*) The variation of vertical wall deflection with wall-station number at early times. Surface position at: —, $t = 0.001$ s; ——, $t = 0.002$ s; –·–, $t = 0.003$ s; – – –, $t = 0.004$ s. (*b*) The variation of vertical wall deflection with wall-station number at later times. (The pressure pulse left the compliant wall at $t = 0.0035$ s.) Surface position at: —, $t = 0.010$ s; ——, $t = 0.011$ s; –·–, $t = 0.012$ s. (*c*) The variation of wall-energy with time. —, E_S; ——, E_K; –·–, E_T; – – –, W_V.

been established. These may be compared with the equivalent undamped responses seen in figures 2(*a*) and 2(*b*). It is immediately obvious that damping is very effective in the removal of the constituent of flexural response to the pressure-pulse whilst not impairing the eventual hydroelastic development of the divergence mode. This is clearly seen when the energy records, figure 4(*c*) (damped wall) and figure 2(*c*) (undamped wall) are compared. Disregarding the greater energy absorbed from the pressure pulse by the undamped wall, the continuing important contribution to the wall energy, after the pulse has left, of E_K in the case of the undamped wall is evidence of the persistence of flexural response. This detracts from the formation of a pure critical (divergence) mode which is reflected in the lower growth rates of the instability. The damped wall, in contrast, quickly shows an elimination of flexural response (giving almost negligible values for E_K) and so adopts the shape of the critical mode at an earlier time; the smoother mode then shows higher growth rates. It may therefore seem that damping promotes divergence instability so supporting the Class A categorization. This is an erroneous inference; damping serves only to expedite the formation of the divergence mode through the removal of flexural response. Once the mode is established, the destabilization is caused by reversible energy transfers and continues to be more properly described as a Class C disturbance.

How can these results be reconciled to the findings of experimental work? Gad-el-Hak *et al.* (1984) clearly demonstrate divergence instability when their viscoelastic wall is exposed to a (turbulent) boundary-layer flow. However, a similar experiment but using an almost elastic wall reported in Gad-el-Hak (1986*a*), shows the wall to

be destabilized by a completely different mode. A fast elastic wave provides the critical instability; this mode is identified as Class B TWF. McMichael *et al.* (1980) have also recorded TWF of a low-damping tensioned membrane subjected to a turbulent boundary-layer flow, having first identified divergence instability and then postponed its onset (by increasing the wall tension) to flow speeds higher than those in which the main investigation was concentrated.

Since there was no evidence of divergence on Gad-el-Hak's elastic wall, he concluded that damping was an essential property for the realization of divergence. Carpenter & Garrad (1986) pointed out that for an elastic surface it is TWF that gives the critical instability; the presence of damping shifts (or can remove completely) the onset of TWF to higher flow speeds than the onset flow speed of divergence. Thus divergence becomes the critical instability. That the damping is not an essential wall property for the occurrence of divergence has also been shown in the present work. Furthermore, the work of McMichael *et al.* (1980) provides another 'zero-damping' situation in which TWF precedes divergence with increasing flow speed. Nevertheless, in this case divergence instability was observed at higher flow speeds. Therefore, one is left wondering why, at higher flow speeds, the TWF of Gad-el-Hak's elastic wall did not give way to the more potent divergence instability. A possible answer emerges from the present results when the travelling pressure pulse is used as the initial excitation. It has been seen in figures 2 (*a*, *b*, *d*) and 4 (*a*, *b*) that divergence only sets in after the pressure pulse has left the trailing edge of the surface. The surface is then able to adopt the particular hydroelastic mode that is unstable in divergence. The turbulent boundary layer used in Gad-el-Hak's 'zero-damping' experiments could be imagined to be providing a stream of pressure pulses, the flexural response to which prevents the wall from adopting the divergence mode. However, when damping is present, as in the viscoelastic experiments, flexural response is quickly attenuated and the divergence mode can form. It has been noted that in the present work, the effect of damping is to eliminate Class B flexural response and promote the formation of the divergence mode. Of course, once divergence is underway, damping exercises its orthodox function in reducing the growth rate of the instability.

3.3. *Wall response to a single-point impulse*

The initiation of surface motion by a travelling pressure pulse could be regarded as predisposing the phase speed of the resulting disturbance to values associated with the phase speed of the pulse. In order to avoid any preconditioning of wall response, this section allows a disturbance to develop from a point pressure pulse applied only at the start of the response history. In this work the wall is represented by a flexible plate with no spring foundation; this type of wall is chosen so as to make comparisons with the work of Brazier-Smith & Scott (1984) who used a similar configuration, calculating deflection histories by means of transform methods. In particular, Brazier–Smith & Scott were interested in differentiating between convective and absolute instabilities. They found only one true hydroelastic instability that was absolute and was subsequently aligned by Carpenter & Garrad (1986), using travelling-wave methods, with the modal-coalescence-flutter solution of the dispersion equation. Of greater interest, perhaps, was that, at flow speeds below the onset of flutter, there existed an 'upstream-incoming' wave that they described as a convective instability. This was envisioned as a wave originating from a location upstream of the initial point of excitation, only growing as it travelled downstream. A similar analysis carried out by Atkins (1982) showed that damping caused this

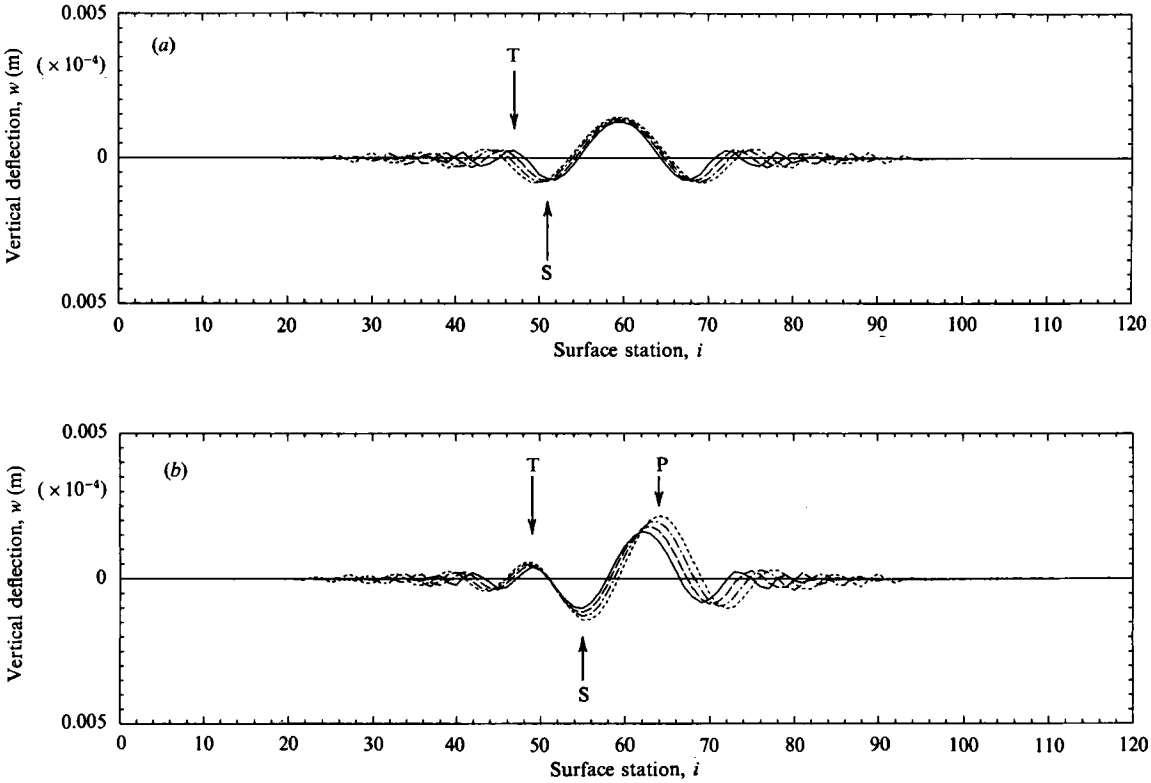

FIGURE 5. The variation of vertical wall deflection with wall-station number after a single-point impulse at $t = 0$ s applied at the wall midpoint ($i = 60$). Surface position at: —, $t = 0.00020$ s; ——, $t = 0.00024$ s; – –, $t = 0.00028$ s; – – –, $t = 0.00032$ s. (*a*) Flow speed, $V = 0$. (*b*) Flow speed, $V = 0.0295$. Wall data: $B = 4904$ Nm, $K_E = 0$, $a = 2.0$ m, $h = 0.01$ m, $\rho_m = 2600$ kg/m^3 and $d = 0$. The fluid density is 1000 kg/m^3.

wave to grow. Carpenter & Garrad have identified this wave as being associated with the divergence wave found using travelling-wave methods and showed that whilst such a wave evidences a positive (downstream) phase speed, it has zero group velocity and is better described as an absolute instability. The results presented here should serve to illustrate the character of such a wave.

In the following, a non-dimensional flow speed, V, is used. It is defined by

$$V = U_\infty \left(\frac{\rho_m h^3}{\pi^4 B} \right)^{\frac{1}{2}}. \tag{3.8}$$

The length to thickness ratio of the undamped flexible plate is 200 and the fluid density is taken as 1000 kg/m^3. Surface motion is initiated by an instantaneous pressure pulse applied at the mid-point of the surface. Figure 5(*a*) shows surface deflections when $V = 0$ for a sequence of time steps shortly after the starting time. At zero flow speed the flexural waves propagate symmetrically outwards from the point of initial excitation. It is noted that the secondary, labelled S, and tertiary, labelled T, (half-wavelength) disturbances have higher wavenumbers and so greater phase speeds. When $V = 0.0295$, the results of figure 5(*b*) are obtained: the primary disturbance, labelled P, evinces growth as it travels downstream. Of more interest is that the upstream secondary disturbance (S) is also travelling downstream and

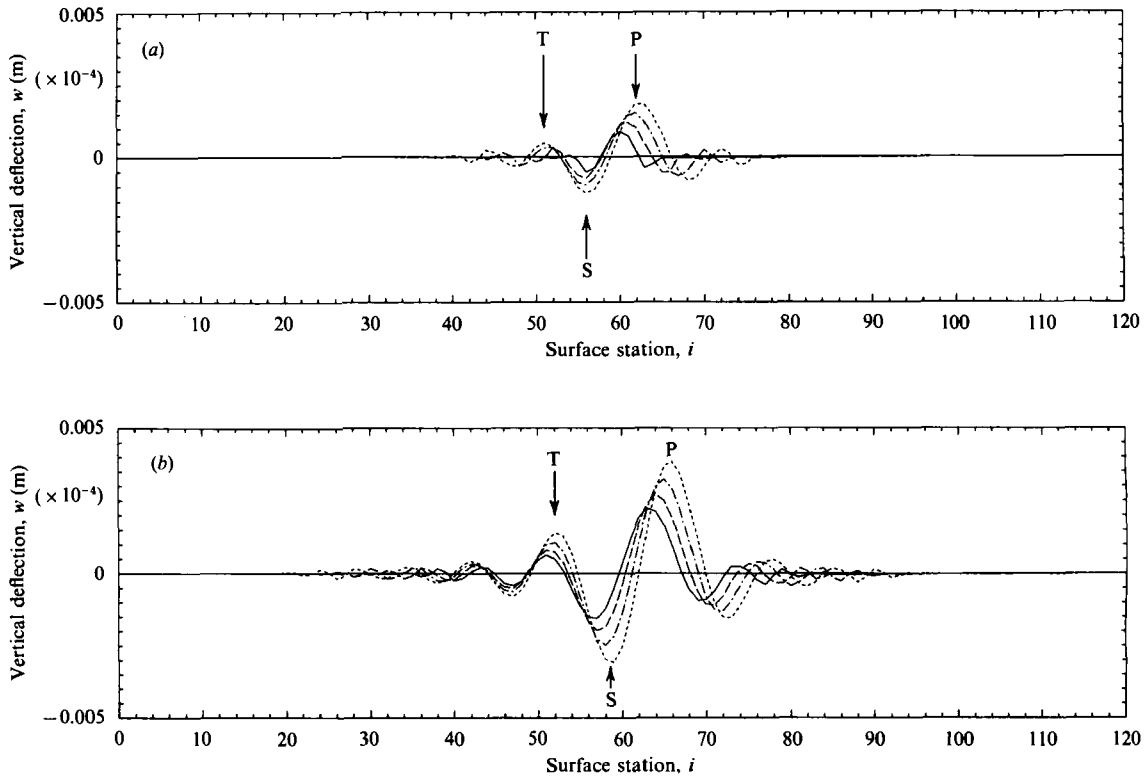

FIGURE 6. The variation of vertical wall deflection with wall-station number after a single-point impulse at $t = 0$ s applied at the wall mid-point ($i = 60$) when the flow speed, V, is 0.0443. (*a*) Early times, surface position at: —, $t = 0.00004$ s; ——, $t = 0.00008$ s; –·–, $t = 0.00012$ s; – – –, $t = 0.00016$ s. (*b*) Later times, surface position at: —, $t = 0.0002$ s; ——, $t = 0.00024$ s; –·–, $t = 0.00028$ s; – – –, $t = 0.00032$ s. Wall and fluid data are as for figure 5.

showing growth before reaching the original point of excitation. This is identified as the 'upstream-incoming' wave. Flexural propagation, modified by hydrodynamic forces, initially spreads energy to locations upstream of the initial point of excitation; thereafter, hydroelastic effects take over and instability sets in as soon as that part of the disturbance wavetrain moves downstream. Again, it is emphasized that this occurs in the absence of damping, thereby reinforcing the combined description of the divergence as an absolute and a Class C instability. The tertiary upstream disturbance (T) continues to propagate upstream at the times shown, its shorter wavelength shows it to be a subcritical (flexural) response at this flow speed.

At a higher flow speed, $V = 0.0443$, figures 6(*a*) and 6(*b*) follows the wall response for a continuous sequence of time steps after the initial excitation. At the later times, plotted in figure 6(*b*), the primary disturbance (P) is showing the more severe modal-coalescence flutter found by Brazier-Smith & Scott, whilst divergence waves are seen in the upstream secondary (S) and tertiary (T) disturbances. Even further upstream, flexural waves are seen to be progressing in the upstream direction. With sufficient time, these too will become hydroelastically unstable. These two figures serve as a summary of the manner in which disturbances (subjected to a sufficiently high flow speed) may first evolve into divergence instability which can then, in turn, become modal-coalescence flutter. Given that modal-coalescence flutter is undeniably a Class C instability this sequence of events adds further support to the characterization of

divergence as a Class C wave. Moreover, these figures illustrate how divergence instability is manifest as a downstream travelling wave and yet can spread to wall locations upstream of the point of initial excitation. The latter effect is typical of an absolute instability. The experiments of Gad-el-Hak *et al.* (1984) show divergence at all locations of the compliant panel. So too in the present work, with sufficient passage of time, instability will come to occupy the entire compliant wall regardless of the location of the initial excitation.

4. Conclusions

A new and versatile method for predicting the hydroelastic response of a passive compliant wall has been developed, tested and then used to conduct an investigation of the two-dimensional, strictly inviscid, instabilities of the wall/flow system. The pre-existence of certain forms of disturbance within the system, commonly assumed in most earlier means of analysis, is not an assumption made in this new method; instead, disturbance forms are allowed to develop subject only to the physics of the system. This work has therefore been able to address the question of causality.

Divergence instability has been shown to exist as a slow downstream-travelling wave. The onset flow speed of this instability is independent of the means of initial excitation; its value may be regarded as a pessimistic prediction because a purely potential flow has been used. For ideal modes, the modification that a boundary layer would impose can be approximately modelled by the application of a factor, $K_p\,\mathrm{e}^{\mathrm{i}\theta_p}$, to the potential-flow result for unsteady pressure. K_p is an overall scaling factor whilst θ_p is the phase-shift angle due to the boundary layer. Since the form of divergence, in the linear regime studied here, has been shown to be nearly sinusoidal, the scaling factors suggested by Kendall (1970) (turbulent boundary layers) and Balasubramanian & Orszag (1983) (laminar boundary layers) could be applied to determine more realistic instability-onset flow speeds. The irreversible energy transfers arising from the pressure phase shift, θ_p, would leave the onset flow speed of divergence unchanged since the wave is static exactly at onset. At higher flow speeds, the pressure phase shift could alter the growth rate of the instability; however, this effect would be secondary since the energy transfers associated with the driving conservative fluid forces always outweigh the irreversible energy transfers for divergence.

At appropriate flow speeds, it has been shown that divergence occurs only after the surface has assumed the shape of a particular critical mode. The wavelength of this mode is determined by the combination of structural and hydrodynamic forces. It is noted that previous methods of analysis are able to predict correctly the divergence-onset flow speed and the critical wavelength (when the ratio of wavelength to surface length is sufficiently small) but yield misleading predictions apropos the nature of the instability. The present simulations of the form of divergence are generally in reasonable agreement with experimental observation. Complete agreement with measured divergence modes is unattainable using the present linear model because experimental results have most often recorded the nonlinear phase of divergence in which structural nonlinearities have overcome hydrodynamic nonlinearities to halt the disturbance growth.

In the travelling-wave analyses of divergence over infinitely long compliant surfaces, wall damping, no matter how light, plays an essential destabilizing role. It slows the surface wave slightly, thereby allowing an energy transfer from the flow to the wall. In contrast, for surfaces of finite length, no matter how long, it is the

existence of edge conditions that facilitate the necessary energy transfer. Thus for finite surfaces, the role of damping seen in the analyses of divergence over infinitely long surfaces, is essentially played by the edge conditions. This allows damping to revert to its more orthodox attenuating role for surface disturbances. Accordingly, for finite compliant walls, damping reduces the growth rate of divergence but leaves its onset flow speed unchanged. Furthermore, the edge conditions also ensure a smooth evolution of modal-coalescence flutter from the divergence instability as the flow speed is increased. After an initiating perturbation, but prior to hydroelastic instability, damping can facilitate the establishment of the necessary instability mode; thereafter, it subtracts from the rate of energy transfer to the wall by the conservative hydrodynamic forces.

In the divergence regime of flows speeds, an increase in the flow speed serves to increase the phase speed of the divergence wave until it evolves into modal-coalescence flutter. The onset flow speed for the latter instability is not clearly defined. Again, damping can be shown to decrease the growth rate of this Class C instability. Further investigation of this flutter has not been pursued since it is known to be strongly three-dimensional.

The response of divergence to damping, the fact that it can spread to wall regions upstream of the location of a point of initial excitation and its relationship to modal-coalescence flutters strongly suggest that divergence is an absolute instability and is also a Class C disturbance.

Although the results presented in this paper have concentrated upon the interaction of a fluid flow with a Kramer-type wall, it is remarked that the general method – that of coupling a boundary-integral flow solution with a solution for wall mechanics – is applicable to other types of finite walls provided that suitable solutions for the wall behaviour are available.

The work described in this paper has been undertaken as part of a research programme at the University of Warwick supported by the Ministry of Defence (Procurement Executive). Most of the work was carried out while A. D. L. was in receipt of an SERC CASE research studentship at the University of Exeter sponsored by the Ministry of Defence. The paper has been prepared during a period when he was supported as a Research Fellow by the MOD.

REFERENCES

Atkins, D. J. 1982 The effect of uniform flow on the dynamics and acoustics of force-excited infinite plates. *Tech. Memo*, AMTE (N) TM 82087. Admiralty Marine Technology Establishment, Teddington, UK.

Balasubramanian, R. & Orszag, S. A. 1983 Numerical studies of laminar and turbulent drag reductions. *NASA Contract Rep.* 3669.

Benjamin, T. B. 1960 Effects of a flexible boundary on hydrodynamic stability. *J. Fluid Mech.* **9**, 513–532.

Benjamin, T. B. 1963 The threefold classification of unstable disturbances in flexible surfaces bounding inviscid flows. *J. Fluid Mech.* **16**, 436–450.

Brazier-Smith, P. R. & Scott, J. F. 1984 Stability of fluid flow in the presence of a compliant surface. *Wave Motion* **6**, 547–560.

Carpenter, P. W. 1990 Status of transition delay using compliant walls. In *Viscous Drag Reduction in Boundary Layers* (ed. D. M. Bushnell & J. M. Hefner), pp. 79–113. AIAA.

Carpenter, P. W. & Gajjar, J. S. B. 1990 A general theory for two- and three-dimensional wall-mode instabilities in boundary layers over isotropic and anisotropic compliant walls. *Theor. Comput. Fluid Dyn.* **1**, 349–378.

CARPENTER, P. W. & GARRAD, A. D. 1985 The hydrodynamic stability of flows over Kramer-type compliant surfaces. Part 1. Tollmien–Schlichting instabilities. *J. Fluid Mech.* **155**, 465–510.

CARPENTER, P. W. & GARRAD, A. D. 1986 The hydrodynamic stability of flows over Kramer-type compliant surfaces. Part 2. Flow-induced surface instabilities. *J. Fluid Mech.* **170**, 199–232.

DANIEL, A. P., GASTER, M. & WILLIS, G. J. K. 1987 Boundary layer stability on compliant surfaces. *British Maritime Technology Ltd., UK, Report*, April 1987.

DOMARADZKI, J. A. & METCALFE, R. W. 1987 Stabilization of laminar boundary layers by compliant membranes. *Phys. Fluids* **30**, 695–705.

DOWELL, E. H. 1975 *Aeroelasticity of Plates and Shells.* Noordhoff.

D'SA, J. M. & DALTON, C. 1990 The dynamic response of compliant materials to an impulsive pressure field. *Intl J. Numer. Meth. Engng* **29**, 811–831.

DUGUNDJI, J., DOWELL, E. & PERKIN, B. 1963 Subsonic flutter of panels on a continuous elastic foundation. *AIAA J.* **1**, 1146–1154.

DUNCAN, J. H., WAXMAN, A. M. & TULIN, M. P. 1985 The dynamics of waves at the interface between a viscoelastic coating and a fluid flow. *J. Fluid Mech.* **158**, 177–197.

ELLEN, C. H. 1973 The stability of simple supported rectangular surfaces in uniform subsonic flow. *Trans. ASME*, E: *J. Appl. Mech.* **95**, 68–72.

EVRENSEL, C. A. & KALNINS, A. 1988 Response of a compliant slab to a viscous incompressible fluid flow. *Trans ASME* E: *J. Appl. Mech.* **55**, 660–666.

GAD-EL-HAK, M. 1985*a* The response of elastic and viscoelastic surfaces to a turbulent boundary layer. *Trans. ASME* E: *J. Appl. Mech.* **53**, 206–212.

GAD-EL-HAK, M. 1986*b* Boundary-layer interactions with compliant coatings: An overview. *Appl. Mech. Rev.* **39**, 511–523.

GAD-EL-HAK, M., BLACKWELDER, R. F. & RILEY, J. F. 1984 On the interaction of compliant coatings with boundary-layer flows. *J. Fluid Mech.* **140**, 257–280.

GARRAD, A. D. & CARPENTER, P. W. 1982 A theoretical investigation of flow-induced instabilities in compliant coatings. *J. Sound Vib.* **84**, 483–500.

GASTER, M. 1987 Is the dolphin a red herring? In *Proc. IUTAM Symp. on Turbulence Management & Relaminarisation, Bangalore, India* (ed. H. W. Liepmann & R. Narasimha), pp. 285–304. Springer.

HANSEN, R. J. & HUNSTEN, D. L. 1974 An experimental study of turbulent flows over compliant surfaces. *J. Sound Vib.* **34**, 297–308.

HANSEN, R. J. & HUNSTEN, D. L. 1983 Fluid-property effects on flow-generated waves on a compliant surface. *J. Fluid Mech.* **133**, 161–177.

HESS, J. L. 1973 Higher order numerical solution of the integral equation for the two-dimensional Neumann problem. *Computer Meth. Appl. Mech Engng* **2**, 1–15.

HESS, J. L. & SMITH, A. M. O. 1966 Calculation of potential flow about arbitrary bodies. *Prog. Aeronaut. Sci.* **8**, 1–138.

HUNT, B. 1978 The panel method for subsonic aerodynamic flows: A survey of mathematical formulations and numerical methods and an outline to the new British Aerospace scheme. In *Computational Fluid Mechanics* (ed. W. Kollmann), pp. 100–165, Hemisphere.

KENDALL, J. M. 1970 The turbulent boundary layer over a wall with progressive waves. *J. Fluid Mech.* **41**, pp. 259–281.

KRAMER, M. O. 1960 Boundary-layer stabilisation by distributed damping. *J. Am. Soc. Naval Engrs* **72**, 25–33; *J. Aero/Space Sci.* **27**, 69.

LANDAHL, M. T. 1962 On the stability of a laminar incompressible boundary-layer over a flexible surface. *J. Fluid Mech.* **13**, 609–632.

LUCEY, A. D. 1989 Hydroelastic instability of flexible surfaces. PhD. thesis, University of Exeter, UK.

LUCEY, A. D., CARPENTER, P. W. & DIXON, A. E. 1991 The rôle of wall instabilities in boundary-layer transition over compliant walls. In *Proc. Boundary Layer Transition and Control, Cambridge, UK, April 1991.* pp. 35.1–35.10. Royal Aeronautical Society.

MCMICHAEL, J. M., KLEBANOFF, P. S. & MEASE, N. E. 1980 Experimental investigation of drag on a compliant surface. In *Viscous Drag Reduction* (ed. G. R. Hough). *AIAA Prog. Astro. Aero.*, vol. 72, pp. 410–438.

METCALFE, R. W., BATTISTONI, F., EKROOT, J. & ORSZAG, S. A. 1991 Evolution of boundary layer flow over a compliant wall during transition to turbulence. In *Proc. Boundary Layer Transition and Control, Cambridge, UK, April 1991*, pp. 36.1–36.14. Royal Aeronautical Society.

PURYEAR, F. W. 1962 Boundary-layer control drag reduction by compliant surfaces. *US Department of Navy, David Taylor Basin Rep.* 1668.

RILEY, J. R., GAD-EL-HAK, M. & METCALFE, R. W. 1988 Compliant coatings. *Ann. Rev. Fluid Mech.* **20**, 393–420.

SEN, P. K. & ARORA, D. S. 1988 On the stability of a laminar boundary-layer flow over a flat plate with a compliant surface. *J. Fluid Mech.* **197**, 201–240.

WEAVER, D. S. & UNNY, T. S. 1971 The hydroelastic stability of a flat plate. *Trans. ASME* E: *J. Appl. Mech.* **37**, 823–827.

WILLIS, G. J. K. 1986 Hydrodynamic stability of boundary layers over compliant surfaces. Ph.D thesis, University of Exeter, UK.